Monatshefte für Chemie - Chemical Monthly
https://doi.org/10.1007/s00706-019-02507-2

ORIGINAL PAPER

Design and synthesis of sulfur cross-linked 1,3,4-oxadiazole-nitro(furan/thiophene)-propenones as dual inhibitors of inflammation and tuberculosis: molecular docking and Hirshfeld surface analysis

Vishwanath Turukarabettu[1,2] · Balakrishna Kalluraya[1] · Monika Sharma[3]

Received: 15 July 2019 / Accepted: 8 October 2019

Abstract

A series of 3-[5-nitro(furan/thiophene)-2-yl]-1-aryl-3-(5-aryl-1,3,4-oxadiazol-2-ylthio)prop-2-en-1-one derivatives was synthesized and studied with the aim of developing dual inhibitors of multidrug-resistant tuberculosis and inflammation. The in vivo anti-inflammatory activity results showed excellent inhibition of rat paw edema. The methoxybenzene/nitrofuryl derivative of title compounds showed 83% inhibition of inflammation during 2–6 h after carrageenan injection. All compounds showed anti-tuberculosis activity at MIC of 50 μg/cm^3. The molecular docking studies revealed that the oxadiazole and nitrofuran groups played a significant role in the inhibiting site of the enzymes COX1, COX2, 5-LOs, and InhA by forming hydrogen bonding with Tyr 385, Ser 530, Tyr 467, and Tyr 158 amino acid residues, respectively. The novel compounds are active antibacterial agents with potential inhibition on *E. coli* bacteria. The toxicity results showed good percentage viability of human kidney cell lines with IC_{50} value greater than 100 μg/cm^3 concentration. The Hirshfeld surface analysis and electrostatic potential map of compound showed good intermolecular contacts and hydrogen bonding donor and acceptor potential.

Graphic abstract

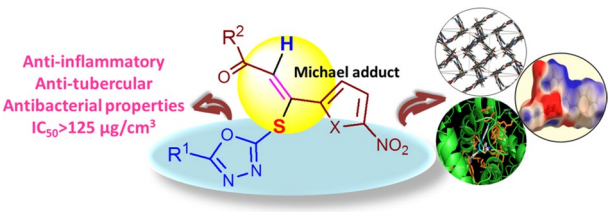

Keywords Michael addition · Alkynes · Carbonyl compounds · Protein · Hydrothiolation · Toxicity

Introduction

Non-steroidal drugs are widely used for the treatment of pain, fever, and inflammation. The prominent side effect of non-steroidal drug is formation of gastric or intestine ulcers and hemorrhage, in addition to the suppression of prostaglandin biosynthesis from arachidonic acid by inhibiting the enzyme cyclooxygenases (COX). The adverse side effects may be controlled by an inhibitor of 5-lipoxygenase (5-LOs) [1–3]. The 1,3,4-oxadiazoles are found to be the

Electronic supplementary material The online version of this article (https://doi.org/10.1007/s00706-019-02507-2) contains supplementary material, which is available to authorized users.

✉ Balakrishna Kalluraya
bkalluraya@gmail.com

[1] Department of Chemistry, Mangalore University, Mangalagangothri 574199, India

[2] Department of Materials Science, Mangalore University, Mangalagangothri 574199, India

[3] Department of Chemical Sciences, IISER, Mohali 140306, India

Published online: 30 October 2019

best remedies against inflammation due to their dual mechanism for inhibition of both COX and LOs [4–12]. In chronic tuberculosis, exacerbated inflammation leads to severe lung tissue necrosis and the promotion of mycobacterial dissemination and transmission [13]. Anti-inflammatory drugs are currently used for therapy in most severe life-threatening forms of tuberculosis such as meningitis and pericarditis, while antibiotics are used to kill the bacteria [13, 14]. The sulfur linked 1,3,4-oxadiazole-propenone derivatives also showed promising potency against *M. tuberculosis* [15]. Pyrazinamide, isoniazid, ethambutol, and rifampicin are few antitubercular drugs which are known to be first-line antituberculosis drugs. The increasing resistance to these first-line drugs, leading to multidrug-resistant tuberculosis, has resulted in the need for second-line drugs. These second-line drugs are less potent and more toxic compared to the first-line drugs [16]. Nitrofurantion (**I**), nifuroxazide (**II**), and furamizole (**III**) are nitrofuran-containing drugs which possess antibacterial properties. The 5-Nitrofuroyl moiety attached to several other chemical motifs **IV**–**VI** was found to be active against multidrug-resistant *M. tuberculosis* and non-toxic [17] (Fig. 1). Therefore, a combination of nitrofuryl moiety and sulfur-linked 1,3,4-oxadiazole-propenone derivative may result in a dual role with anti-inflammatory and antimycobacterial activity.

Considering the above findings, and in continuation of our study on bioactive heterocycles [18–21], we have designed a series of 1,3,4-oxadiazole-propenone derivatives with nitrofuryl/nitrothienyl moiety as promising dual inhibitors of inflammation and *Mycobacterium tuberculosis*. The significance of this study is sulfur cross-linking of 5-aryl-1,3,4-oxadiazole and nitrofuran/nitrothiophene-propenone pharmacophores, which are known for their wide range of biological activity [4–12]. This cross linking was achieved through the Michael-type addition of 5-aryl-1,3,4-oxadizole-2-thiols **6a**, **6b** to acetylenic ketones **5a**–**5h** containing nitrofuran/nitrothiophene in benzene under reflux condition (Schemes 1, 2).

The in vitro antitubercular activity was carried out on all synthesized compounds. The in vivo anti-inflammatory analysis was performed on compounds **7a**, **7b**, **7c**, **7h**, and **7i**, which showed active ligand–protein interactions in the docking study. The antibacterial activity was studied by using agar well diffusion method. The toxicity study on human

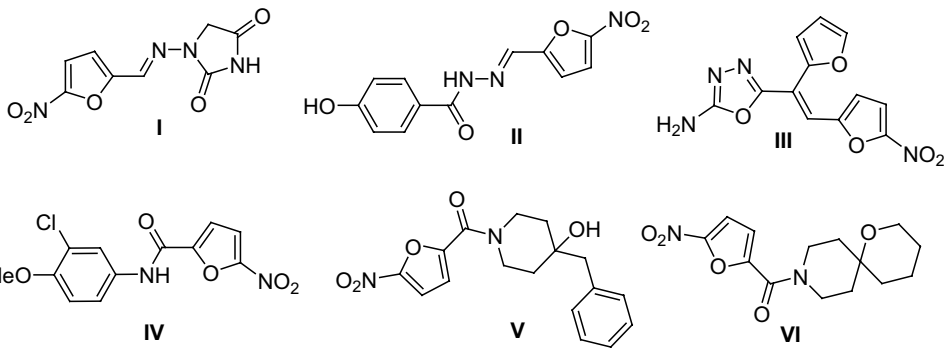

Fig. 1 Antibacterial drugs containing a nitrofuryl moiety

Scheme 1

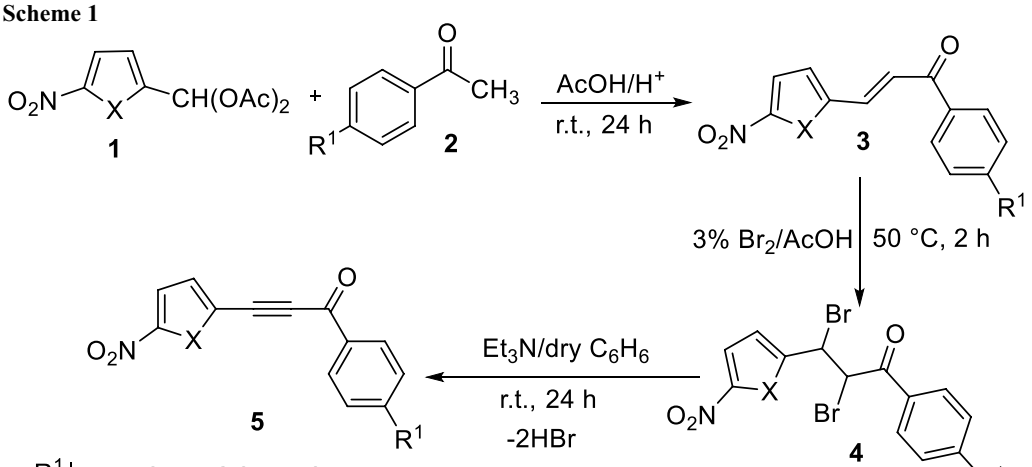

R^1	H	CH_3	OCH_3	Cl	F
X=O	**5a**	**5b**	**5c**	**5d**	-
X=S	**5e**	**5f**	**5g**	-	**5h**

Scheme 2

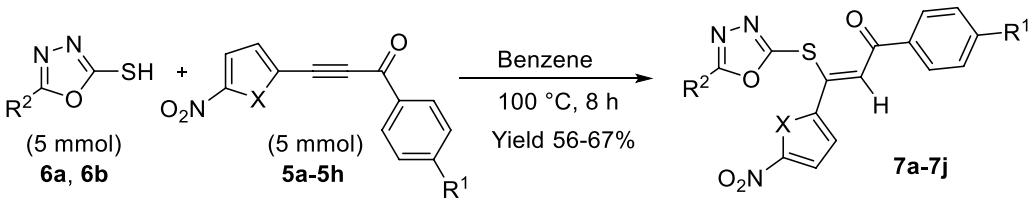

kidney cell line was carried out for active anti-inflammatory compounds to establish the IC_{50} level by in vitro MTT assay.

Results and discussion

Chemistry

The synthetic route for acetylenic ketones **5a**–**5h** is given in Scheme 1. The acid-catalyzed condensation of 5-nitro-2-(furyl/thienyl)methyl diacetate **1** and *para* substituted acetophenone gave corresponding propenones **3** in acetic acid. Bromination of propenones in acetic acid and their subsequent dehydrobromination in dry benzene employing triethylamine as base gave acetylenic ketones **5a**–**5h**.

Further, the hydrothiolation of acetylenic ketones **5a**–**5h** with compounds **6a**, **6b** is shown in Scheme 2. The reaction proceeded via Michael-type addition to give only *Z* regioisomer (as confirmed by single crystal XRD) of the propenone rather than a mixture of *E*/*Z* isomers, as seen in the literature protocol for hydrothiolation of internal alkynes [22, 23]. The ^{1}H NMR spectrum of crude compound was recorded which showed resonance signals corresponding to the single isomer. The presence of electron-withdrawing nitro group on acetylenic ketone causes the negative inductive effect on alkyne carbon and facilitates the nucleophilic attack of sulfur at the β carbon of alkyne. Thus, the sp^3 hybridized sulfur atom bridges the propenone and 1,3,4-oxadiazole moieties. The newly synthesized 3-[5-nitro(furan/thiophen)-2-yl]-1-phenyl-3-(5-aryl-1,3,4-oxadiazol-2-ylthio)prop-2-en-1-ones **7a**–**7j** were characterized by FT-IR, ^{1}H NMR, ^{13}C NMR, mass spectra, and elemental analysis. The yields and melting point data are given in Table 1.

The FT-IR spectra of compounds **7a**–**7j** were recorded in KBr. The characteristic absorption bands at 1585–1600 cm^{-1} are due to C=C stretching vibrations. The C=O stretching was observed at 1624–1635 cm^{-1} as a sharp absorption band. The asymmetric and symmetric stretching of the nitro group was observed around 1460 and 1375 cm^{-1}, respectively. In the ^{1}H NMR spectra of compounds **7a**–**7j**, the alkene proton at α carbon resonated as a singlet at $\delta = 7.57$–8.27 ppm. The ^{13}C NMR spectra of compounds **7a**–**7j** showed a peak at $\delta = 186$–188 ppm, corresponding to the carbonyl carbon. The HMBC spectra showed ^{1}H–^{13}C signal correlations

Table 1 Series of (*Z*)-3-[5-nitro(furan/thiophen)-2-yl]-1-aryl-3-(5-aryl-1,3,4-oxadiazol-2-ylthio)prop-2-en-1-one derivatives **7a**–**7j**

Compd.	R^1	R^2	X	Yield/%	M.p./°C
7a	C_6H_5	H	O	66	198–202
7b	C_6H_5	CH_3	O	64	214–216
7c	C_6H_5	OCH_3	O	60	200–202
7d	C_6H_5	Cl	O	65	229
7e	C_6H_5	CH_3	S	60	198–200
7f	C_6H_5	OCH_3	S	57	179–181
7g	C_6H_5	F	S	62	174
7h	*o*-HO-C_6H_4	H	S	67	182–184
7i	*o*-HO-C_6H_4	CH_3	O	56	171–173
7j	*o*-HO-C_6H_4	OCH_3	S	58	191–193

and no alkenyl isomeric protons were observed. Elemental analyses (C, H, N) results were found to be in good agreement (±0.3%) with the calculated values. The *m/z* values of 'calculated exact mass' of compounds **7a**–**7j** are ($[M+1]^+$): 420.06, 434.08, 450.08, 454.03, 450.06, 466.05, 454.03, 452.04, 450.08, 482.05; and the 'experimental accurate mass' data are: 419.50, 434.00, 449.50, 453.40, 449.50, 465.55, 454.20, 451.45, 449.55, 481.45. The *m/z* data is a result of single measurements, and differences in exact and accurate masses are due to instrument errors [24]. Detailed spectral and analytical data are given in the experimental section.

Single crystal XRD data

The single crystal data were collected by X-ray diffraction technique for 3-(5-nitrofuran-2-yl)-1-phenyl-3-[5-(*p*-tolyl)-1,3,4-oxadiazol-2-ylthio]prop-2- en-1-one (**7b**) (CCDC No. 1499538). The ORTEP diagram of compound **7b** drawn with thermal displacement ellipsoids at 50% probability level is given in Fig. 2. The single crystal was characterized as follows: crystal system: monoclinic; space group: $P2_1/C$; $a = 18.724(1)$ Å, $b = 6.982(1)$ Å, $c = 16.667(16)$ Å; $\alpha = 90°$, $\beta = 113.84°$, $\gamma = 90°$; $V = 1993.0(4)$ Å^3; $Z = 4$; $\mu = 0.204$ mm^{-1}; $\rho_{calc\ -} = 1.444$ Mg m^{-3}; $F_{(000)} = 896.0$; $2.378 \le \theta \le 26.429$; $R = 0.0412$; $wR = 0.1296$.

A portion of the molecule, comprising the nitrofuran ring, benzoyl ring, and the central segment (O1/C7-C9)

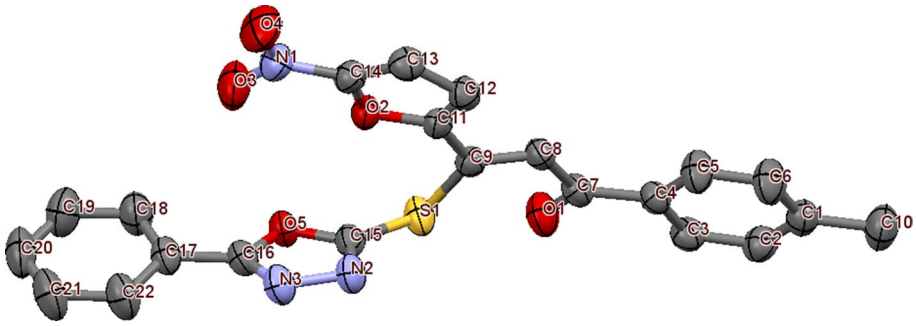

Fig. 2 The ORTEP diagram of the compound **7b** viewed along the *c*-axis

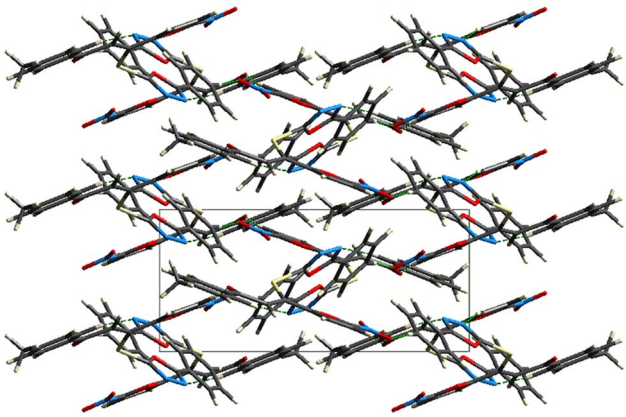

Fig. 3 The crystal packing structure of compound **7b** viewed along the *a*-axis

connecting the two rings, was almost planar as indicated by the dihedral angles, 2.25(8)° (between nitrofuran and benzoyl rings), 12.08(10)° (benzoyl rings and the central segment), and 13.94(10)° (nitrofuran ring and the central segment). The oxadiazole ring (C15/N2–N3/C16/O5) made dihedral angles of 12.41(10)°, 58.39(9)°, and 59.32(8)° with phenyl (C17–C22), nitrofuran (C11–C14/O2), and benzoyl (C1–C6) rings, respectively. The molecule was twisted at sulfur atom (S1) with torsion angle C8–C9–S1–C15 being equal to 154.46(5)°. The torsion angle of the alkene segment H8–C8–C9–S1 was found to be 178.84(6)°. The crystal packing structure was drawn using CrystalExplorer [25, 26] and viewed along the *a*-axis of unit cell as shown in Fig. 3. The crystal structure was stabilized by C–H···O type of intermolecular contacts and their intermolecular hydrogen bond geometries are given in Table 2.

Hirshfeld surface analysis

The short contacts in single crystal of compound **7b** were identified by Hirshfeld surface analysis [27, 28]. The Hirshfeld surfaces and their corresponding 2D-finger plots are shown in Fig. 4. In the 2D fingerprint plot, d_i is the closest internal distance from a given point on the Hirshfeld surface

Table 2 The intermolecular hydrogen bonding interactions in **7b** crystal

–D–H··A–/Å	D –H/Å	H··A/Å	D··A/Å	D-H··A/°
C12–H12···N2	1.083	2.450	3.533 (6)	159.83
C20–H20···O4	1.083	2.606	3.689 (2)	175.72
C5–H5···N3	1.083	2.446	3.529 (2)	134.03

to the nearest nucleus and d_e is the closest external contacts from the surface. The higher percentages of inter-contacts are arrived for C–H (19.8%), H–H (27.9%), N–H (10.1%), and O–H (20%) interactions along with other short contacts which are shown below the respective plots in Fig. 4.

The electrostatic potential of compounds **7b** (Fig. 5) was mapped using wave function STO-3G basis set with Hartree–Fock theory over the range of ± 0.025 au [28]. The positive electrostatic potential (blue) region represents the hydrogen donor potential and the negative electrostatic potential (red) region represents the hydrogen bond acceptors. The volume of electrostatic potential for compound **7b** was found to be 489.65 $Å^3$.

The Hirshfeld analysis results indicated that the compounds possess hydrogen bond donors and acceptors, which would extend the possible interactions with biomolecules for good biological activity.

In vivo anti-inflammatory activity and molecular docking studies

The in vivo anti-inflammatory activity study was conducted by carrageenan-induced rat right hind paw edema method [29]. The test results are presented in Table 3, as mean paw volume ± SEM, $n = 6$. Compounds **7a**, **7b**, **7c**, and **7i**, which contain nitrofuryl moiety showed moderate to good anti-inflammatory activity than compound **7h**, which contains nitrothiophene moiety, as indicated by the control in the paw edema after 2 h of carrageenan injection. The compounds **7b**, **7c**, and **7i** showed 66.65%, 85.71%, and 80.94% of inhibition during the 2nd hour of study, respectively. Interestingly, among the tested

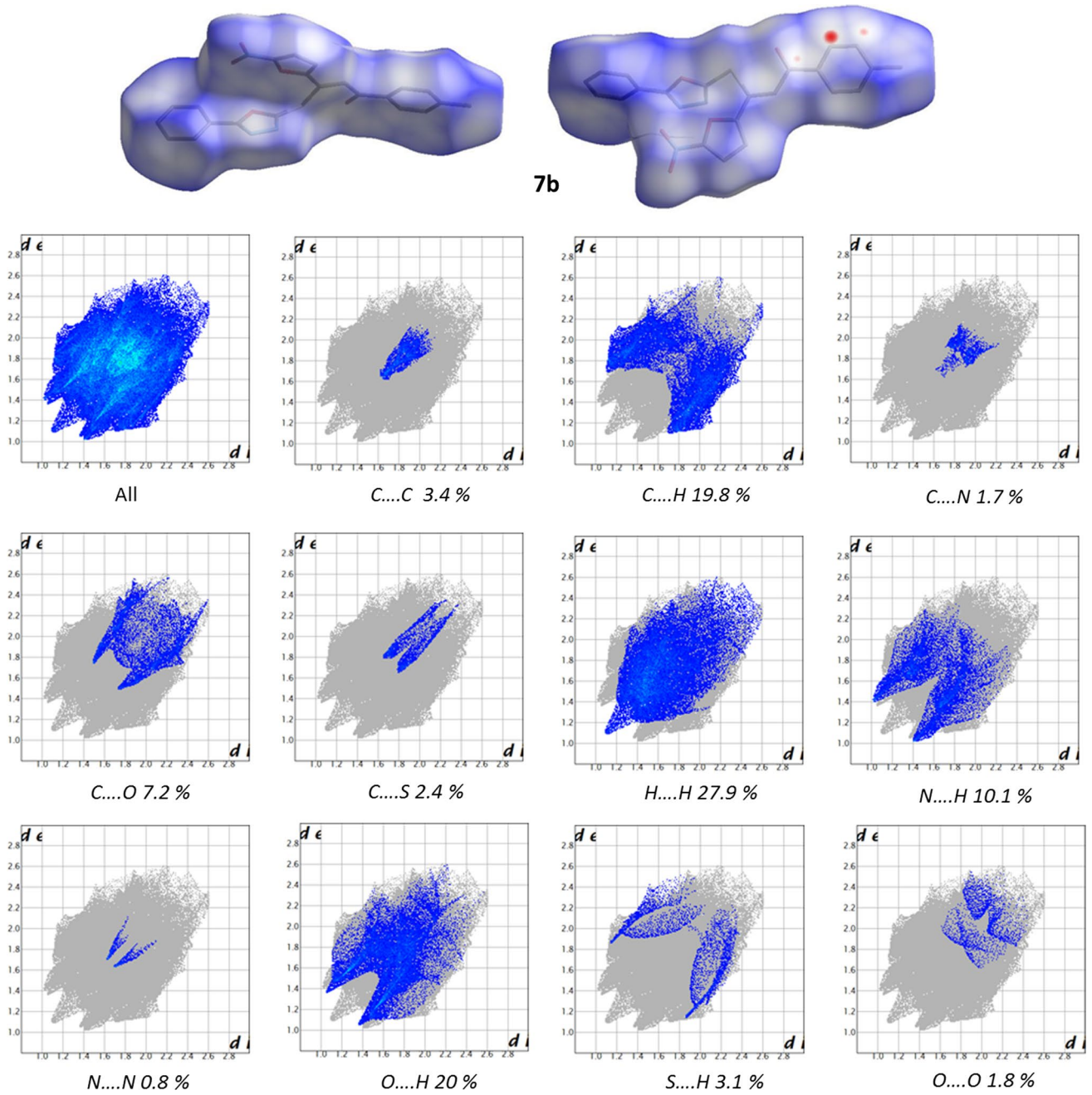

Fig. 4 Hirshfeld surfaces mapped with d_{norm} ranging from − 0.24 to 1.61 Å and its 2D finger plots visualizing the intercontacts of the compound **7b**

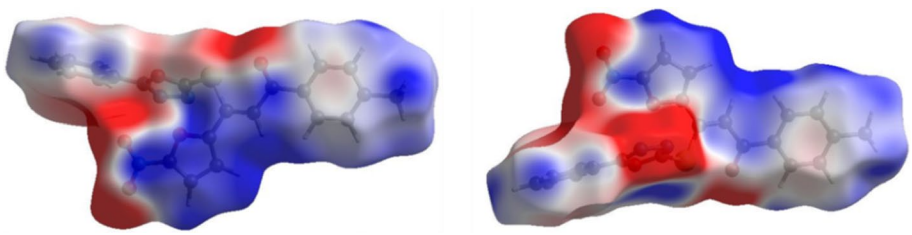

Fig. 5 The electrostatic potential mapped on Hirshfeld surfaces (front and rear view) over a range of ± 0.025 au for compound **7b**

Table 3 Anti-inflammatory activity results of 1,3,4-oxadiazole derivatives as mean increase in paw volume in $cm^3 \pm SEM$ values

Compound	Time/h				
	0	1	2	4	6
Control	0.466 ± 0.06	0.716 ± 0.06	0.816 ± 0.040	1.067 ± 0.07	1.167 ± 0.06
Diclofenac	0.450 ± 0.02	0.700 ± 0.02	0.750 ± 0.05	0.600 ± 0.02	0.550 ± 0.22
7a	0.650 ± 0.04	0.883 ± 0.09	0.95 ± 0.04***	1.133 ± 0.01	0.800 ± 0.03***
7b	0.583 ± 0.03	0.826 ± 0.06	0.700 ± 0.05	0.90 ± 0.10	0.883 ± 0.07**
7c	0.500 ± 0.04	0.746 ± 0.08*	0.550 ± 0.04**	0.60 ± 0.02**	0.616 ± 0.04***
7i	0.533 ± 0.02	0.716 ± 0.03	0.600*	0.933 ± 0.06	0.783 ± 0.04***
7h	0.400 ± 0.04	0.65 ± 0.10	0.733 ± 0.07	1.067 ± 0.09	0.750 ± 0.09***

Levels of significance: $*P = 0.05$, $**P < 0.01$, $***P < 0.001$

compounds, **7c** was found to be the most active (83.3%) for the inhibition of paw edema (Table S1 of ESI).

The *in silico* molecular docking results of compounds **7b**, **7c**, and **7i** docked with COX1 and COX2 protein molecule showed hydrogen bonding network in the same pocket as that of reference drug diclofenac. The compounds are shown as ball and stick models. The protein is shown in cartoons for best docked conformations and as lines in the enlarged pictures. The diclofenac is shown in magenta color and labeled as DIF 701. The best conformation of **7b** with COX1 and their hydrogen bonding interactions are shown in Fig. 6.

The ligands showed their stable conformation in the active site of COX1 with amino acid residues Tyr 385, Tyr 355, Ser 530, Gly 526, Val 349, Phe 381, Trp 381, Leu 384, and Val 349, which is a key requirement for anti-inflammatory activity as seen in several studies [4]. The compound **7b** exhibited the highest gliding score of − 49.79 kJ/mol. The 1,3,4-oxadiazole nitrogen formed a hydrogen bonding with Tyr 385 and the nitro group formed polar interactions with Ser 530. The compounds **7c** and **7i** showed the same active pocket for stable binding conformation as that of **7b** (Fig. S1 of ESI) and hydrogen bonding interactions with Ser 530 and Tyr 385. The docking scores for **7c** and **7i** were − 44.35 kJ/mol and − 46.86 kJ/mol, respectively.

The active site of COX2 protein for the ligands **7b**, **7c**, **7i**, and diclofenac was identified as Ser 530, Tyr 355, Tyr 385, Tyr 115, His 90, Leu 352, Leu 531, Phe 518, Gly 526, and Val 349. The compound **7b** exhibited the highest gliding score of − 53.56 kJ/mol. The hydrogen bonding interactions were found between His 90 and the nitro group, and Tyr 355 and 1,3,4-oxadiazole (Fig. 7). The compound **7c** showed hydrogen bond with Tyr 355 at nitrogen of the 1,3,4-oxadiazole ring with docking score − 53.17 kJ/mol. Similarly, the compound **7i** formed hydrogen bonding interactions with Tyr 355 at the nitro group and oxygen of the furan ring (Fig. S2 of ESI) with a gliding score of − 46.44 kJ/mol.

The docking experiments of 5-LOs with compounds **7b**, **7c**, and **7i** showed moderate ligand–protein interactions, as indicated by their low binding energy compared to the COX studies. The active binding pocket for compound **7b** in the protein 5-LOs was identified as Ser 444, Tyr 467, Gln 546, Thr 363, Ala 450, and Arg 367, with polar interactions (Fig. 8). The gliding score value was found to be − 19.25 kJ/mol. Similarly, the compounds **7c** and **7i** showed gliding score of − 23.43 kJ/mol and − 30.96 kJ/mol, respectively,

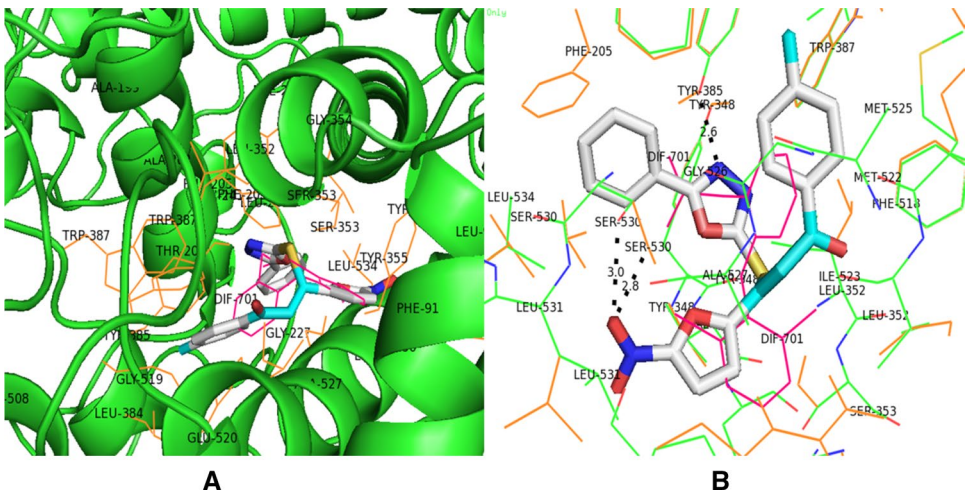

Fig. 6 **a** The docked view of compound **7b** with diclofenac in the active site of COX1 (3N8Y) and **b** hydrogen bonding interaction

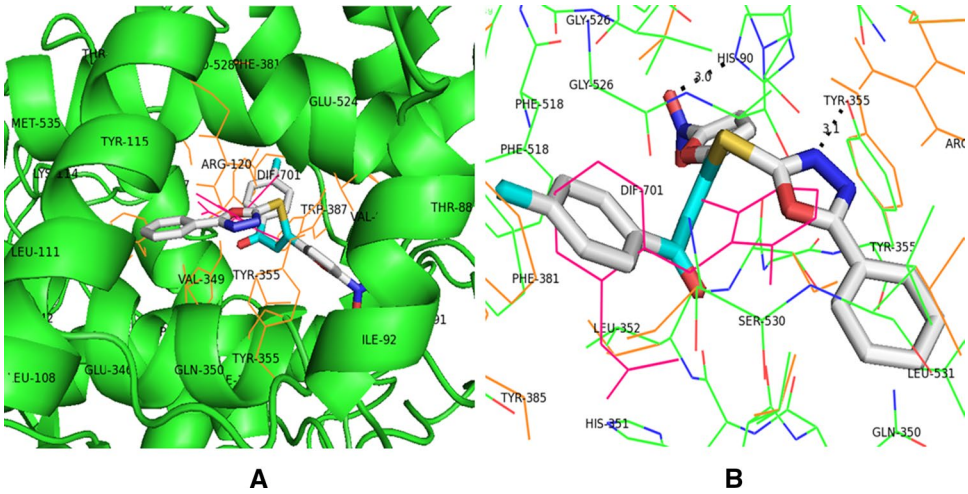

Fig. 7 **a** The docking pocket of compound **7b** with re-docked diclofenac in COX2 (1PXX) and **b** the hydrogen bonding interaction

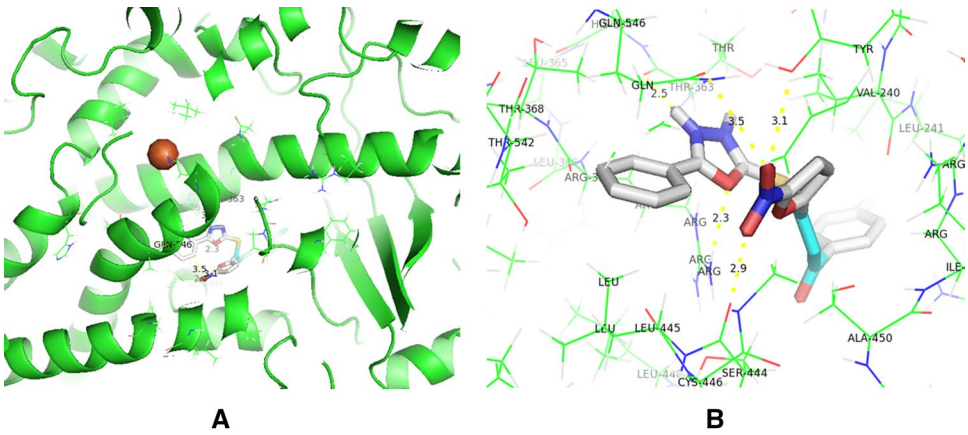

Fig. 8 **a** The docked view of compound **7b** in 5-LOs (3O8Y) and **b** their hydrogen bonding interactions

in the active binding pocket of protein as shown in Fig. S3 of ESI.

Antimycobacterial activity

Microplate Alamar Blue assay (MABA) methodology was used for antitubercular study [30]. The in vitro antimycobacterial results showed that all compounds **7a**–**7j** are active against multidrug-resistant *M. tuberculosis* (ATCC 35835) at a minimum inhibitory concentration of 50 µg/cm^3 compared to the standard drug streptomycin which showed an MIC value of 6.25 µg/cm^3. The docking analysis of compound **7c** showed that the compound has a stable conformation in the InhA active site of protein (Fig. 9). The Tyr 158 and oxidized form of nicotinamide adenine dinucleotide (NAD+, shown in yellow) are active sites for the antimycobacterial activity as referred to in the literature [16]. The compound formed hydrogen bonding network and gliding score of − 43.93 kJ/mol in the vicinity of amino acids: Tyr 158, Phe 149, Phe 97, Met 98, Met 103, Met 161, Met 199, Ser 200, Ala 198, His 265, and Asp 150. This active site and hydrogen bonding with Tyr 158 seem to be a conserved feature among all the InhA-inhibitor compounds synthesized so far [31]. In addition to this, the nitro group and carbonyl group formed three polar co-ordination bonds with NAD+.

Antibacterial activity

The antibacterial activity of synthesized compounds was determined by agar well diffusion method [32] and the results were represented as diameter of zone of inhibition of bacterial growth in millimeters. The following test microorganisms were used: Gram-positive bacteria *Bacillus subtilis* ATCC 33712, *Staphylococcus aureus* ATCC 25923, and Gram-negative bacteria *Escherichia coli* ATCC 25922 and *Klebsiella pneumoniae* ATCC 700603. The antibacterial activity results of test compounds are given in Table 4.

All compounds showed moderate to good antibacterial activity compared to the standard drug ampicillin for the tested bacterial strains. The compounds showed very good activity against Gram-negative bacteria *E. coli,* and among the tested compounds **7f** was found to be the most effective.

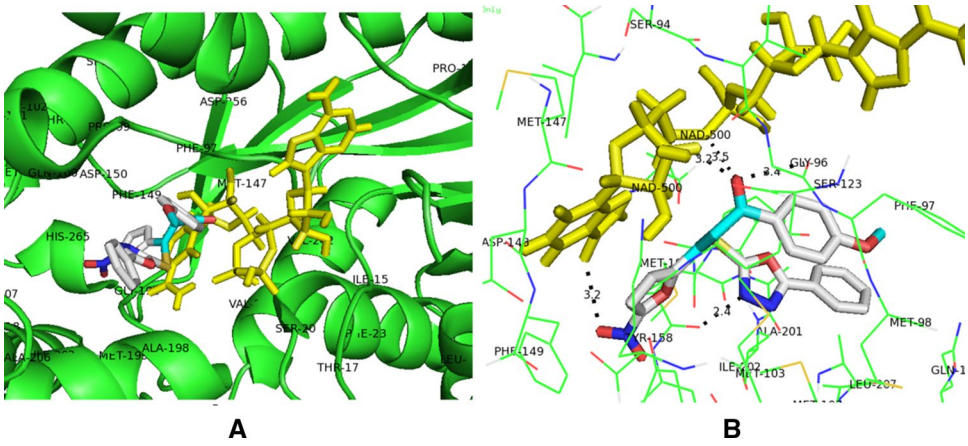

Fig. 9 **a** The docked view of compound **7c** in the active site of MTb (4TZK) and **b** the hydrogen bonding interaction

Table 4 Antibacterial activity data of (*Z*)-3-[5-nitro(furan/thiophen)-2-yl]-1-aryl-3-(5-aryl-1,3,4-oxadiazol-2-ylthio)prop-2-en-1-ones **7a–7j**

Test compounds	Antibacterial activity at 10 mg/cm^3 (Zone of inhibition/mm)			
	B. subtilis	*S. aureus*	*E. coli*	*K. pneumoniae*
Control	–	–	–	–
Ampicillin	21 ± 0.1	26 ± 0.1	12	29 ± 0.2
7a	10	20 ± 0.2	–	12 ± 0.3
7b	12 ± 0.6	21 ± 0.3	10	12 ± 0.1
7c	15 ± 0.2	12 ± 0.1	10 ± 0.2	12 ± 0.2
7d	10 ± 0.3	14 ± 0.1	15 ± 0.1	10
7e	11 ± 0.2	12	9 ± 0.1	–
7f	20	11 ± 0.3	23 ± 0.1	8 ± 0.1
7g	15 ± 0.4	9 ± 0.3	15 ± 0.2	–
7h	10 ± 0.6	8 ± 0.2	10 ± 0.5	8 ± 0.4
7i	15 ± 0.1	13	15	18 ± 0.2
7j	20 ± 0.1	11	–	13 ± 0.3

The compound **7j** was found to be most active against *B. subtilis*, and **7a** and **7b** were active against *S. aureus*. In general, compounds carrying alkyl and alkoxy substituents have shown good antibacterial activity.

Toxicity studies

The compounds **7b**, **7c**, and **7i** which showed good anti-inflammatory and antituberculosis activity were tested for their toxicity by in vitro MTT assay [33]. The human kidney cell line HEK293 was used for the study. The test results are documented in Table 4 as the percentage viability of kidney cell lines against various concentrations of compounds and the standard drug mitomycin C at 500 µg/cm^3 concentration (Fig. 10).

The toxicity study revealed that the test compounds **7b**, **7c**, and **7i** showed good IC_{50} value of 133.65 µg/cm^3, 243.02 µg/cm^3, and 274.03 µg/cm^3, respectively. Interestingly, the compounds **7c** and **7i** showed better percentage

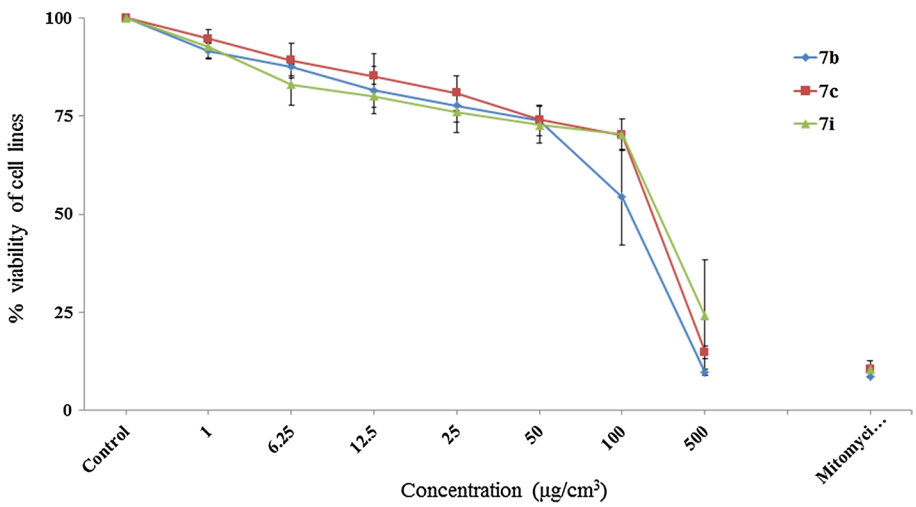

Fig. 10 The percentage viability of HEK293 cell lines

viability at 500 µg/cm^3 concentration (14.89% and 24.12%, respectively) to that of the standard drug (10.46%).

Conclusion

In summary, a series of 1,3,4-oxadiazole-propenone derivatives were prepared and evaluated for their biological activity. The in vivo anti-inflammatory study indicated that the nitrofuran derivatives possess good inhibition of inflammation and the highest inhibition was observed between the 2nd to 6th hour for **7c**. The docking studies showed that the target compounds are both COX1 and COX2 active site binders as well as moderate inhibitors of 5-LOs. All compounds exhibited antituberculosis activity and were found to be active InhA blockers. The antibacterial activity study showed that the compounds are moderate to good antibacterial agents. Compounds **7c** and **7i** were found to be least toxic to the human kidney cell lines, with IC_{50} value of greater than 240 µg/cm^3, in comparison with the standard drug mitomycin 500. The Hirshfeld surface analysis showed that the compounds possess hydrogen bond donors and acceptors which would extend the possible interactions with biomolecules for good biological activity. These findings indicated that synthesized nitrofuran/nitrothiophene containing 1,3,4-oxadiazole-propenone derivatives would exhibit anti-inflammatory as well as antimicrobial activity. Further study in the structure–activity relationship of these lead compounds would benefit in the development of drugs for treatment of severe tuberculosis associated with inflammation.

Experimental

All chemicals were procured commercially, and further purification was done wherever needed. The melting point of newly synthesized compounds was determined using Innovative DTC-967A instrument. IR spectra were recorded on a Shimadzu FTIR 157 spectrophotometer. The ^{1}H and ^{13}C NMR spectra were recorded on Agilent VNMRS-400 MHz NMR spectrometer using TMS as internal standard. Mass spectra were recorded using Shimadzu 8030-LCMS/MS mass spectrometer. Elemental analysis was carried out on Vario-EI elementar III model elemental analyzer. The single crystal data were collected on Bruker D8 Venture Photon 100 CMOS X-ray diffractometer at 293 K.

General procedure for preparation of acetylenic ketones 5a–5h

To a well-stirred solution of 5-nitro-2-(furyl/thienyl)methyl diacetate **1** (5 mmol) in 20 cm^3 glacial acetic acid, substituted acetophenone **2** (5 mmol) and 0.5 cm^3 of conc. H_2SO_4 were added. The reaction mixture was stirred for 1 h and kept aside at room temperature. The propenone crystals **3** formed were collected by filtration and washed with ethanol. The crude product **3** (5 mmol) was dissolved in 20 cm^3 glacial acetic acid by heating. 30% v/v bromine solution was added drop by drop until bromination was complete. The reaction mixture was stirred for 2 h and kept aside overnight. The α,β-dibromochalcones **6** formed were filtered, washed with ethanol, and recrystallized from glacial acetic acid. The dibromochalcone **4** (5 mmol) was taken in a round-bottomed flask and 25 cm^3 of dry benzene was added. To this, triethylamine (6 mmol) was added and the flask was closed with a lid. The mixture was stirred for 4 h and the separated triethylammonium hydrobromide filtered off. The filtrate was roto-evaporated and the solid separated was collected by filtration and further purified by recrystallization from ethanol. The compounds were characterized by reference to their melting point [34, 35] and the data are given in ESI.

General procedure for synthesis of compounds 7a–7j

The acetylenic ketone **5a**–**5h** (5 mmol) and 5-aryl-1,3,4-oxadiazole-2-thiol **6a**, **6b** (5 mmol) were taken in a round-bottomed flask containing 50 cm^3 of dry benzene. A water-cooled condenser was attached to the round-bottomed flask and the reaction mixture was refluxed on an oil bath at 100 °C under atmospheric pressure conditions. The progress of the reaction was monitored by TLC (ethylacetate and petroleum ether 1:3). The solution was then rota-evaporated to remove the excess solvent. The solid obtained was recrystallized from DMF/ethanol mixture.

(*Z*)-3-(5-Nitrofuran-2-yl)-1-phenyl-3-(5-phenyl-1,3,4-oxadiazol-2-ylthio)prop-2-en-1-one (7a, $C_{21}H_{13}N_3O_5S$) Yellow crystalline; IR (KBr): $\bar{\nu}$ = 1629 (C=O), 1595 (C=C), 1541 (C=N), 1469 (NO_2 assym. str.), 1377 (NO_2 sym. str.), 970 (C–S) cm^{-1}; ^{1}H NMR ($CDCl_3$): δ = 8.0 (d, 2H, J = 8.8 Hz), 7.97 (s, 1H, = C–H), 7.46–8.95 (m, 8H), 7.23 (d, 1H, J = 3.6 Hz, NF-4H), 6.87 (d, 1H, J = 3.6 Hz, NF-3H) ppm; ^{13}C NMR ($CDCl_3$): δ = 188.6 (C=O), 151.3, 136.4, 134.1, 132.9, 129.1, 129.0, 128.7, 128.2, 126.9, 122.9, 115.1, 115, 112.6 ppm; MS: m/z = 419.50 ([M + 1]$^+$).

3-(5-Nitrofuran-2-yl)-1-phenyl-3-[5-(*p*-tolyl)-1,3,4-oxadiazol-2-ylthio]prop-2-en-1-one (7b, $C_{22}H_{15}N_3O_5S$) Yellow crystalline; IR (KBr): $\bar{\nu}$ = 1627 (C=O), 1521 (C=N) cm^{-1}; ^{1}H NMR (DMSO-d_6): δ = 8.20 (s, 1H, = C–H), 7.88 (d, 2H, J = 8.4 Hz), 7.76 (d, 1H, J = 4 Hz, NF-4H), 7.58 (d, 1H, J = 5.6 Hz, NF-3H), 7.56–8.08 (m, 5H), 7.42 (d, 2H, J = 8.4 Hz), 2.49 (s, 3H, CH_3) ppm; ^{13}C NMR (DMSO-d_6): δ = 188.9 (C=O), 152.7, 144.6, 137.2, 135.5, 134.7, 130.5,

130.2, 129, 128.3, 127.8, 126.1, 117.3, 114.1, 111.8, 21.2 (CH_3) ppm; MS: $m/z = 434$ ($[M+1]^+$).

1-(4-Methoxyphenyl)-3-(5-nitrofuran-2-yl)-3-(5-phenyl-1,3,4-oxadiazol-2-ylthio)prop-2-en-1-one (7c, $C_{22}H_{15}N_3O_6S$) Yellow crystalline; IR (KBr): $\bar{\nu} = 1637$ (C=O), 1597 (C=C), 1516 (C=N), 966 (C-S) cm^{-1}; ^1H NMR ($CDCl_3$): $\delta = 7.93$ (s, 1H, =C-H), 7.02 (d, 1H, $J = 4$ Hz, NF-4H), 6.99–8.07 (m, 9H), 6.83 (d, 1H, $J = 3.6$ Hz, NF-3H), 3.90 (s, 3H, OCH_3) ppm; ^{13}C NMR (DMSO-d_6): $\delta = 188.7$ (C=O), 166.7, 160.7, 151.7, 145.4, 135.6, 134.0, 132.8, 130.1, 129.9, 129.5, 129.4, 127.0, 123.1, 114.6, 52.4 (OCH_3) ppm; MS: $m/z = 449.50$ ($[M+1]^+$).

1-(4-Chlorophenyl)-3-(5-nitrofuran-2-yl)-3-(5-phenyl-1,3,4-oxadiazol-2-ylthio)prop-2-en-1-one (7d, $C_{21}H_{12}ClN_3O_5S$) Yellow crystalline; IR (KBr): $\bar{\nu} = 1627$ (C=O), 1585 (C=C), 1537, 1523 (C=N), 970 (C–S) cm^{-1}; ^1H NMR (DMSO-d_6): $\delta = 8.27$ (s, 1H, =C-H), 7.61 (d, 1H, $J = 4$ Hz, NF-4H), 7.46–8.26 (m, 9H), 7.43 (d, 1H, $J = 5.6$ Hz, NF-3H) ppm; ^{13}C NMR (DMSO-d_6): $\delta = 189$ (C=O), 170.5, 165.7, 155.8, 155.5, 135.3, 135.2, 132.5, 130.7, 131.9, 130.7, 129.3, 127, 125, 120.5, 115.2 ppm; MS: $m/z = 453.40$ ($[M+1]^+$), 455.40 ($[M+3]^+$) (^{37}Cl), with peak intensity ratio of 3:1.

3-(5-Nitrothiophen-2-yl)-1-phenyl-3-[5-(*p*-tolyl)-1,3,4-oxadiazol-2-ylthio]prop-2-en-1-one (7e, $C_{22}H_{15}N_3O_4S_2$) Yellow crystalline; IR (KBr): $\bar{\nu} = 1637$ (C=O), 1589 (C=C), 1548 (C=N), 950 (C–S) cm^{-1}; ^1H NMR (DMSO-d_6): $\delta = 8.09$ (s, 1H, =C-H), 8.04 (d, 2H, $J = 8.4$ Hz), 7.99 (d, 1H, $J = 4.4$ Hz, NT-4H), 7.79 (d, 2H, $J = 7.6$ Hz), 7.53–7.60 (m, 3H), 7.50 (d, 1H, $J = 4.4$ Hz, NT-3H), 7.37 (d, 2H, $J = 8$ Hz), 2.38 (s, 3H, CH_3) ppm; ^{13}C NMR (DMSO-d_6): $\delta = 188.7$ (C=O), 166.7, 160.3, 151.8, 146.9, 145.4, 138.7, 134, 132.9, 130.2, 130, 129.9, 129.5, 129.3, 126.9, 122.8, 21.7 ppm; MS: $m/z = 449.50$ ($[M+1]^+$).

1-(4-Methoxyphenyl)-3-(5-nitrothiophen-2-yl)-3-(5-phenyl-1,3,4-oxadiazol-2-ylthio)prop-2-en-1-one (7f, $C_{22}H_{15}N_3O_5S_2$) Yellow crystalline; IR (KBr): $\bar{\nu} = 1637$ (C=O), 1595 (C=C), 1546, 1520 (C=N), 900 (C-S) cm^{-1}; ^1H NMR ($CDCl_3$): $\delta = 8.01$ (d, 2H, $J = 8$ Hz), 7.85 (d, 2H, $J = 8.4$ Hz), 7.65 (d, 1H, $J = 4.4$ Hz, NT-4H), 7.57 (s, 1H, =C–H), 7.43–7.57 (m, 3H), 7.15 (d, 1H, $J = 4$ Hz, NT-3H), 6.99 (d, 2H, $J = 8.4$ Hz, ArH), 3.90 (s, 3H, OCH_3) ppm; ^{13}C NMR ($CDCl_3$): $\delta = 186.7$ (C=O), 164.4, 146.3, 132.3, 131, 129.4, 129.1, 128.3, 127.3, 126.7, 122.8, 114.3, 55.6 (OCH_3) ppm; MS: $m/z = 465.55$ ($[M+1]^+$).

1-(4-Fluorophenyl)-3-(5-nitrothiophen-2-yl)-3-(5-phenyl-1,3,4-oxadiazol-2-ylthio)prop-2-en-1-one (7g, $C_{21}H_{12}FN_3O_4S_2$) Brown needles; IR (KBr): $\bar{\nu} = 1629$ (C=O), 1600 (C=C), 1541 (C=N), 902 (C–S) cm^{-1}; ^1H NMR (DMSO-d_6): $\delta = 8.14$ (s, 1H, =C–H), 8.04 (d, 1H, $J = 4.4$ Hz, NT-4H), 7.54 (d, 1H, $J = 4.4$ Hz, NT-3H), 7.42–7.84 (m, 9H) ppm; ^{13}C NMR (DMSO-d_6): $\delta = 187.7$ (C=O), 166.7 ($^1J_{C\text{-}F} = 230$ Hz, Ar C-F), 164.8, 160.2, 151.9, 146.8, 139.5, 133.2 ($^3J_{C\text{-}F}$, 12.4 Hz, Ar C-F), 133, 132.5 ($^2J_{C\text{-}F} = 39$ Hz, Ar C-F), 130.2, 129.7, 128.8, 126.9, 122.8, 116.7, 116.5 ppm; MS: $m/z = 454.2$ ($[M+1]^+$).

3-[5-(2-Hydroxyphenyl)-1,3,4-oxadiazol-2-ylthio]-3-(5-nitrothiophen-2-yl)-1-phenylprop-2-en-1-one (7h, $C_{21}H_{13}N_3O_5S_2$) Yellow crystalline; IR (KBr): $\bar{\nu} = 1633$ (C=O), 1589 (C=C), 1543 (C=N), 900 (C-S) cm^{-1}; ^1H NMR ($CDCl_3$): $\delta = 9.69$ (s, 1H, OH), 7.98 (s, 1H, =C-H), 7.95 (d, 2H, $J = 8$ Hz), 7.25 (d, 1H, $J = 4$ Hz, NT-4H), 6.94–7.60 (m, 9H), 6.86 (d, 1H, $J = 4$ Hz, NT-3H), 2.44 (s, 3H, CH_3) ppm; ^{13}C NMR ($CDCl_3$): $\delta = 186.2$ (C=O), 166, 158.7, 157.2, 150.5, 147.1, 135.7, 133.4, 132.3, 131.4, 130.8, 129.8, 129.5, 127.5, 120.1, 117.5, 117.2, 114.2, 110.2 ppm; MS: $m/z = 451.45$ ($[M+1]^+$).

3-[5-(2-Hydroxyphenyl)-1,3,4-oxadiazol-2-ylthio]-3-(5-nitrofuran-2-yl)-1-(*p*-tolyl)prop-2-en-1-one (7i, $C_{22}H_{15}N_3O_6S$) Yellow crystalline; IR (KBr): $\bar{\nu} = 3309$ (O–H), 1624 (C=O), 1591 (C=C), 1543 (C=N), 894 (C–S) cm^{-1}; ^1H NMR ($CDCl_3$): $\delta = 9.69$ (s, 1H, OH), 7.95 (d, 2H, $J = 8$ Hz, ArH), 7.98 (s, 1H, =C-H), 7.58 (d, 1H, $J = 8$ Hz, ArH), 7.43 (t, 1H, $J = 7.2$ Hz, 6.8 Hz, salicyl-4H), 7.32 (d, 2H, $J = 8.4$ Hz, ArH), 7.25 (d, 1H, $J = 4$ Hz, NF-4H), 7.06 (d, 1H, $J = 8.4$ Hz, ArH), 6.93 (t, 1H, $J = 7.6$ Hz, 8 Hz, salicyl-5H), 6.86 (d, 1H, $J = 4$ Hz, NF-3H), 2.44 (s, 3H, CH_3), ppm; ^{13}C NMR ($CDCl_3$): $\delta = 188.5$ (C=O), 167, 157.5, 159.9, 151.3, 145.5, 135.2, 134.5, 132.1, 130.2, 129.5, 129, 126.5, 120.1, 118.5, 115.2, 113.2, 107.2, 22 (CH_3) ppm; MS: $m/z = 449.55$ ($[M+1]^+$).

3-[5-(2-Hydroxyphenyl)-1,3,4-oxadiazol-2-ylthio]-1-(4-methoxyphenyl)-3-(5-nitrothiophen-2-yl)prop-2-en-1-one-(7j, $C_{22}H_{15}N_3O_6S_2$) Yellow crystalline; IR (KBr): $\bar{\nu} = 3327$ (O–H), 1624 (C=O), 1589 (C=C), 1544 (C=N), 898 (C–S) cm^{-1}; ^1H NMR ($CDCl_3$): $\delta = 9.66$ (s, 1H, OH), 8.01 (d, 2H, $J = 7.2$ Hz, ArH), 7.69 (d, 1H, $J = 2$ Hz, NT-4H), 7.60 (s, 1H, =C–H), 7.17 (d, 1H, $J = 2$ Hz, NT-3H), 7.06 (d, 1H, $J = 8.8$ Hz, salicyl-3H), 6.93–7.52 (m, 8H), 6.93 (t, 1H, $J = 7.2$ Hz, 6.8 Hz, salicyl-4H), 3.90 (s, 3H, OCH_3) ppm; ^{13}C NMR ($CDCl_3$): $\delta = 186.7$ (C=O), 166.4, 164.5, 159.6, 157.5, 146.2, 134.3, 131.1, 129.3, 128.3, 128, 127.8, 126.3, 120.1, 117.8, 114.3, 107.2, 55.6 (OCH_3) ppm; MS: $m/z = 481.45$ (M^+).

In vivo anti-inflammatory activity

Male Wistar rats were taken, fasted for 12 h, and given free access to water. Since the synthesized compounds were less

soluble in 0.1% Tween 80–saline solution than in diclofenac sodium, the compounds were administered at higher dosage, orally at 100 mg/kg body weight by gavage to each group of six animals. Diclofenac sodium at a dose of 10 mg/kg body weight was used as a standard anti-inflammatory agent. The negative control group received 0.1% Tween 80 in saline solution. Acute inflammation was produced by sub-plantar injection of 0.1 cm^3 of 1% suspension of carrageenan in normal saline in the right hind paw just below the tibiotarsal junction of the rats 1 h after the oral administration of the test compounds. The paw volume was measured by a plethysmometer at 0 h, 1 h, 2 h, 4 h, and 6 h after the carrageenan injection. The anti-inflammatory activity of the test compounds and the standard reference drug was determined using the formula:

$$\text{Percentage of anti-inflammatory activity} = 1 - \left(\frac{V_t}{V_c}\right) \times 100,$$

where V_t is the mean increase in paw volume in rats treated with test compounds and V_c represents the mean increase in paw volume in the control group of rats.

In vitro antimycobacterial activity

Sterile deionized water (200 mm^3) was added to all outer perimeter wells of sterile 96-well plates to minimize evaporation of medium in the test wells during incubation. The 96-well plate received 100 mm^3 of the Middlebrooks 7H9 broth and serial dilution of compounds were made directly on plate. The final drug concentrations tested were from 0.2 to 100 µg/cm^3. Plates were covered and sealed with parafilm and incubated at 37 °C for 5 days. 25 mm^3 of freshly prepared 1:1 mixture of Alamar Blue reagent and 10% Tween 80 was added to the plate and incubated again for 24 h. A blue color in the well was interpreted as no bacterial growth, and pink color was scored as growth. The MIC was defined as lowest drug concentration which prevented the color change from blue to pink.

Antibacterial activity

The overnight-grown culture was prepared by inoculating a loopful of culture to broth media. The test samples were prepared at a concentration of 10 mg/cm^3 by dissolving in DMSO followed by sonication. Five millimeter diameter wells on agar plates were made using a sterile cork-borer. 20 mm^3 of test sample/standard at the concentration of 10 mg/cm^3 was loaded on to the wells. All bacterial cultures were incubated at 37 °C and observed for the zone of inhibition. The diameter of the zone of inhibition was measured.

Molecular docking

The molecular docking studies were carried out using Autodocksuite-4.2.5.1 molecular docking software [36]. The aspirin acetylated COX1 (3N8Y with X-ray resolution 2.6 Å), diclofenac bound to COX2 (1PXX with X-ray resolution 2.9 Å), human 5-LOs (3O8Y with X-ray resolution 2.38 Å), and 1-cyclohexyl-*N*-(3,5-dichlorophenyl)-5-oxopyrrolidine-3-carboxamide (CDOC) bound MTb (4TZK with X-ray resolution 1.62 Å) were the protein molecules obtained from the protein data bank [31, 37–39]. The structure of protein molecules was simplified by removing HETATOMS, co-crystallized molecules, and water molecules. The force field parameters and topology files for all ligands were generated using PRODRUG server [40]. Flexible torsions were defined using AutoTors provided with AutoDock suite. The reference drug molecule (diclofenac for COX1 and COX2; CDOC for MTb) was redocked together with the docked compounds in the inhibitor binding site. PyRx 0.8 interface was used with grid box size 86×85×80, spacing 0.361 and assigning three degrees of freedom. The Lamarckian genetic algorithm was employed with ten conformations for each ligand and the best pose with the highest binding energy was considered as the stable docking site and visualized using PyMOL Molecular Graphics System [41].

Toxicity study

The cells were taken in a confluent cell line flask and trypsinized. Phosphate buffer saline wash was given twice and centrifuged. The cells were resuspended in 10% fetal bovine serum medium and counted using a hemocytometer. These cells (3000–10,000) were plated to 96-well plates and incubated at 37 °C in a CO_2 incubator for 24 h. Then the medium was discarded from 96-well plates. The drug solution was prepared in a series of concentrations from 1 to 500 µg/cm^3 in serum and added to different test groups. The test plates were incubated again for 48 h. 20 mm^3 of MTT dye (5 mg/mm^3) was added to all wells and incubated for 4 h. 100 mm^3 of DMSO was added to all the wells and shaken well. The absorbance of all the test samples was recorded at 540 nm.

Acknowledgements The authors are grateful to NGSM Institute of Pharmaceutical Sciences Nitte (Deemed to be University) for carrying out animal studies and USIC Mangalore University for spectral data.

References

1. Rajak H, Kharya M, Mishra P (2007) Yakugaku Zasshi 127:1757
2. Vane JR (1971) Nature 231:232
3. Vane JR, Bakhle Y, Botting R (1998) Annu Rev Pharmacol Toxicol 38:97

4. Abdel-Aziz AAM, Abou-Zeid LA, ElTahir KEH, Ayyad RR, El-Sayed MAA, El-Azab AS (2016) Eur J Med Chem 121:410
5. Omar FA, Mahfouz NM, Rahman MA (1996) Eur J Med Chem 31:819
6. Shetgiri NP, Nayak BK (2005) Indian J Chem B 44:1267
7. Golgolab H, Lalezari I, Hosseini L, Hosseini-Gohari L (1973) J Heterocycl Chem 10:387
8. Singh AK, Lohani M, Parthsarathy R (2013) Iran J Pharm Res 12:319
9. Jayashankar B, Rai KML, Baskaran N, Sathish HS (2009) Eur J Med Chem 44:3898
10. Arshad M (2014) Int J Pharm Sci Res 5:1124
11. Akhter M, Husain A, Azad B, Ajmal M (2009) Eur J Med Chem 44:2372
12. Bharathi D, Hemalatha S, Devadas G, Kumar PR, Shanmugasundaram P, Aanandhi MV (2010) Int J Chemtech Res 2:1867
13. Biá-Ventura TL, Calixto SD, Vieira B, D'Souza AMT, Mello MVP, Rodrigues CR, Miranda LS, D'Souza ROMA, Leal ICR, Lasunskaia EB, Muzitano MF (2015) Molecules 20:8072
14. Thwaites G, Fisher M, Hemingway C, Scott G, Solomon T (2009) J Infect 59:167
15. Jha KK, Samad A, Kumar Y, Shaharyar M, Khosa R, Jain J, Bansal S (2009) Iran J Pharm Res 8:163
16. Tatar E, Karakus S, Kucukguzel SG, Okullu SO, Unubol N, Kocagoz T, De Clercq E, Andrei G, Snoeck R, Pannecouque C, Kalayci S, Sahin F, Sriram D, Yogeeswari P, Kucukguzel I (2016) Biol Pharm Bull 39:502
17. Krasavin M, Lukin A, Vedekhina T, Manicheva O, Dogonadze M, Vinogradova T, Zabolotnykh N, Rogacheva E, Kraeva L, Sharoyko V, Tennikova TB, Dar'in D, Sokolovich E (2019) Eur J Med Chem 166:125
18. Ramaprasad GC, Kalluraya B, Kumar BS, Hunnur RK (2010) Eur J Med Chem 45:4587
19. Kalluraya B, Aamir S, Shabaraya AR (2012) Eur J Med Chem 54:597
20. Girisha KS, Kalluraya B, Narayana V (2010) Eur J Med Chem 45:4640
21. Isloor AM, Kalluraya B, Pai KS (2010) Eur J Med Chem 45:825
22. Movassagh B, Shaygan P (2006) Ark Online J Org Chem 12:130
23. Omar MT, Basyouni MN (1974) Bull Chem Soc Jpn 47:2325
24. Brenton AG, Godfrey AR (2010) J Am Soc Mass Spectrom 21:1821
25. Wolff SK, Grimwood DJ, McKinnon JJ, Jayatilaka D, Spackman MA (2007) Crystal Explorer 3.0, University of Western Australia, Perth, Australia
26. Spackman MA, McKinnon J (2002) J Cryst Eng Commun 4:378
27. Soman R, Sujatha S, Arunkumar C (2014) J Fluorine Chem 163:16
28. Spackman MA, McKinnon JJ, Jayatilaka D (2008) CrystEngComm 10:377
29. Winter CA, Risely EA, Nuss GW (1962) Proc Soc Exp Biol 111:544
30. Collins LA, Franzblau SG (1997) Antimicrob Agents Chemother 41:1004
31. He X, Alian A, Stroud R, de Montellano PRO (2006) J Med Chem 49:6308
32. Ansari FL, Nazir S, Noureen H, Miraza B (2005) Chem Biodivers 2:1656
33. Mosmann T (1983) J Immunol Methods 65:55
34. Balakrishna K (1987) Synthesis, characterization and biological activities of some nitrofuran and oxadiazole derivatives. PhD Thesis, Mangalore University, India
35. Alphonsus D (1994) Some contributions to the chemistry of nitrogen and sulphur containing heterocycles. PhD Thesis, Mangalore University, India
36. Morris GM, Huey R, Lindstrom W, Sanner MF, Belew RK, Goodsell DS, Olson AJ (2009) J Comput Chem 16:2785
37. Sidhu RS, Lee JY, Yuan C, Smith WL (2010) Biochemistry 49:7069
38. Rowlinson SW, Keifer JR, Prusakiewicz JJ, Pawlitz JL, Kozak KR, Kalgutkar AS, Stallings WC, Kurumbail RG, Marnett LJ (2003) J Biol Chem 278:45763
39. Gilbert NC, Bartlet SG, Waight MT, Neau DB, Boeglin WE, Brash AR, Newcomer ME (2011) Science 331:217
40. Schuttelkopf AW, van Aalten DMF (2004) Acta Crystallogr D Biol Crystallogr 60:1355
41. The PyMOL Molecular Graphics System, Version 2.0. Schrondinger, LLC